Heat Transfer and Pressure Drop Characteristics of Flat Tube and Louvered Plate Fin Surfaces

A. Achaichia
Research Fellow
T. A. Cowell
Reader
Department of Mechanical and Production Engineering, Brighton Polytechnic, Moulsecoomb, Brighton, UK

■Performance data are presented for a range of flat tube and louvered plate fin surfaces. The Stanton number curves demonstrate characteristics that are consistent with the notion that at high Reynolds number the fluid flow is predominantly parallel to the louvers but that as Reynolds number is reduced the flow direction becomes increasingly determined by the plate fins. This effect causes a flattening of the Stanton number curves as the effective heat transfer configuration changes from "flat plate" to "duct flow." This flattening of the Stanton number curves with reducing Reynolds number is clearly demonstrated to be a genuine effect and not to result from the problems of experimental accuracy that can arise at very low Reynolds number.

The results of other work by Achaichia and Cowell, which uses numerical methods to describe flow through louver arrays, have been used to develop a very simple nondimensional correlating equation for Stanton number. An equation for friction factor has also been developed, but a dimensional form was found to be necessary for it to retain useful accuracy.

Keywords: *augmentation, finned surfaces, forced convection, heat exchangers*

INTRODUCTION

Compact heat transfer surfaces consisting of flat-sided tubes and louvered plate fins of the type shown in Fig. 1 are widely used in industrial and automotive applications where a liquid at relatively low pressure is to be cooled by air. However, very few relevant performance data have been published in the open literature. Kays and London [1] have given data for a few plain variants, with both in-line and staggered tube row arrangements. They give results for a few cases in which the fin is rippled in the airflow direction. Davenport [2] has given data for a related surface—the flat tube and louvered corrugated fin geometry—but it is our experience that these data have limited applicability to the surfaces under study here. The paucity of published information seems to result from the commercial value of any performance data, on the one hand, and the difficulty and cost of manufacturing the many samples needed for a systematic study, on the other.

This paper presents the results of an experimental program to measure the performance of a range of in-line flat tube and louvered plate fin surfaces. The sparse literature on the operating characteristics of louvered surfaces is reviewed in the second section. Then the test surfaces and their mode of manufacture are described. Following that, experimental test equipment is described, and experimental results are presented. The correlating equations derived to express Stanton number and friction factor as functions of Reynolds numbers and the geometrical parameters are presented in the final section.

FLOW PHENOMENA IN LOUVERED FINS

As stated in the introduction, very few performance data are available in the literature. However, a number of authors have considered the operating mechanisms of louvered heat transfer surfaces.

Beauvais [3] used flow visualization on large-scale models to demonstrate that louvers act to realign the airflow in a direction parallel to their own planes. Smith [4] modeled pressure drop through a louvered matrix by treating the matrix as an assembly of flat plates. Agreement to within 15% of the experimental results was claimed. Later attempts to model heat transfer [5] were less successful. Wong and Smith [6] confirmed the validity of using large-scale models for evaluation of these surfaces and also carried out local air velocity measurements that confirmed the flow-directing properties of the louver discovered by Beauvais.

Davenport [7] has presented a comprehensive study of the characteristics of a nonstandard variant of the flat tube and louvered corrugated fin. He repeated the smoke trace measurements of Beauvais and demonstrated that the degree of alignment with the louvers was a function of Reynolds number. At low Re values, realignment would be slight, but at high Re it was almost complete. Davenport conjectured that at low air velocities the developing boundary layers on the louvers

Address correspondence to Dr. T. A. Cowell, Department of Mechanical and Production Engineering, Brighton Polytechnic, Moulsecoomb, Brighton, UK BN2 4GJ.

Experimental Thermal and Fluid Science 1988; 1:147-157

0894-1777/88/$3.50

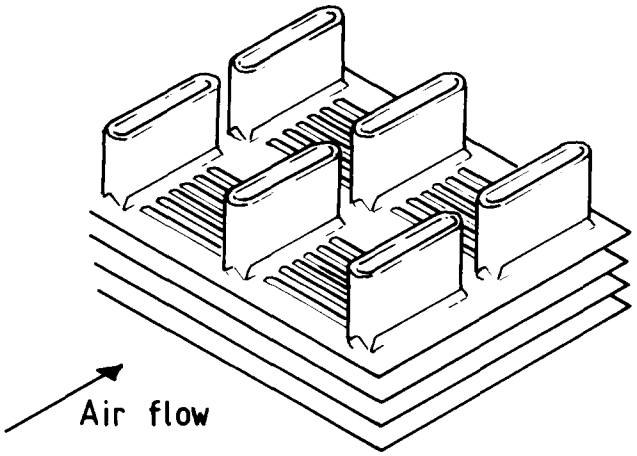

Figure 1. Flat-sided tube and louvered plate fin heat transfer surface.

become sufficiently thick to effectively block off the gaps between louvers. The flow then passes largely straight through the louver array down the gap between fins. Figure 2 shows a section through a typical louver array to illustrate the point. Davenport further conjectured that a flattening of the experimental Stanton number curve as Reynolds number is reduced was due to this same effect. Against this, it has frequently been argued (eg, Shah and Webb [8]) that such flattening of the Stanton number curve is due to experimental error. At the high values of N_{tu} (number of heat transfer units) associated with compact surfaces at low velocity, it is easily shown that the experimental accuracy falls off rapidly as velocity is reduced.

Recent work by Achaichia and Cowell [9, 10] has used numerical methods to model the flow through a simplified two-dimensional louver array. The louvers are assumed to be infinitely thin, and the analysis describes the fully developed periodic flow situation. Under these conditions the theory suggests that Davenport's explanation of his experimental results can indeed be correct. Of particular interest is the way in which the mean fluid flow direction is found to vary with Reynolds number, louver angle, and the ratio of fin pitch to louver pitch. The curves in Fig. 3, taken from Ref. 9, show how at low Re values the mean flow angle is in all cases significantly lower than the louver angle, and that as Re increases the mean flow direction approaches the louver angle to within a few degrees.

SURFACE GEOMETRY

The dimensional details of the geometry are given in Fig. 4. All the samples tested have one or two rows of brass tubes with a fixed tube size (16 × 2 mm), fixed tube longitudinal pitch (20 mm), and a fixed fin depth in the airflow direction (41.6 mm). Copper fin thickness is always 0.05 mm. A total of 23 samples were made with 15 different combinations of values of tube transverse pitch, fin pitch, louver pitch, and louver angle. The values for these variables are given for each of the variants made in Table 1. Values of hydraulic diameter and σ, the ratio of free flow to frontal area, are also given. Two samples each of variants 1–8 were made and tested. In all cases the louvers were extended as close to the tube walls as the manufacturing process would allow. This was to approximately 0.5 mm less than the gap between the walls of adjacent tubes. In all cases the louvered area occupied 74% of the fin depth in the airflow direction, and the louvers were inclined in opposite directions for each tube row. Half-louvers were used at the inlet and outlet to each louver bank.

To manufacture the fins, tools were specially made using the same principles that are applied to the design of roll tolls for large-scale production. The major significant differences were that roll pitch circle diameters were 75 mm rather than the 120–200 mm that is usual with production tooling, and the rolls were hand-operated rather than power-driven. The tooling was found to be capable of producing fins equivalent to those made with high-quality large-scale production tools. More details of the tool design and manufacturing process are given in Ref. 9.

A new tool is required for each value of louver pitch and for each value of tube transverse pitch. This led to the need for a total of five tools. It was found possible to vary the louver angle over the range 20–30° by making small adjustments in the closing of the two rolls. Fin pitch is determined during the assembly of fin and tube into a complete matrix, which involves the lacing of fins onto an array of solder-coated tubes. The assembly is oven-baked to make the solder joints between fin and tube, and then header plates and tanks are fitted to yield

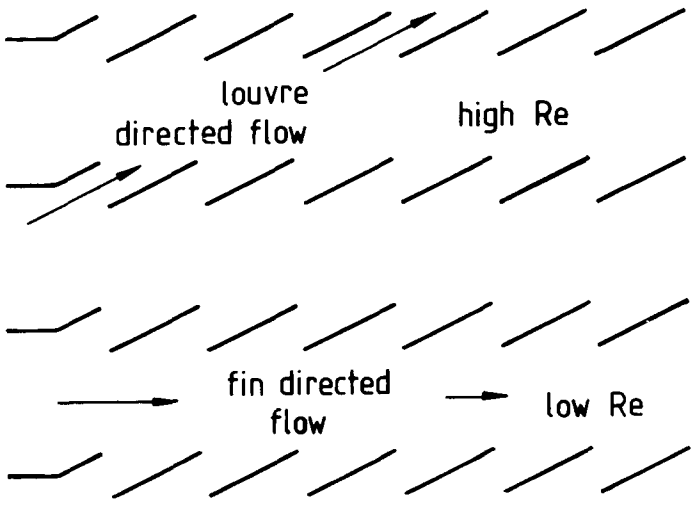

Figure 2. Section through louver array indicating possible flow directions.

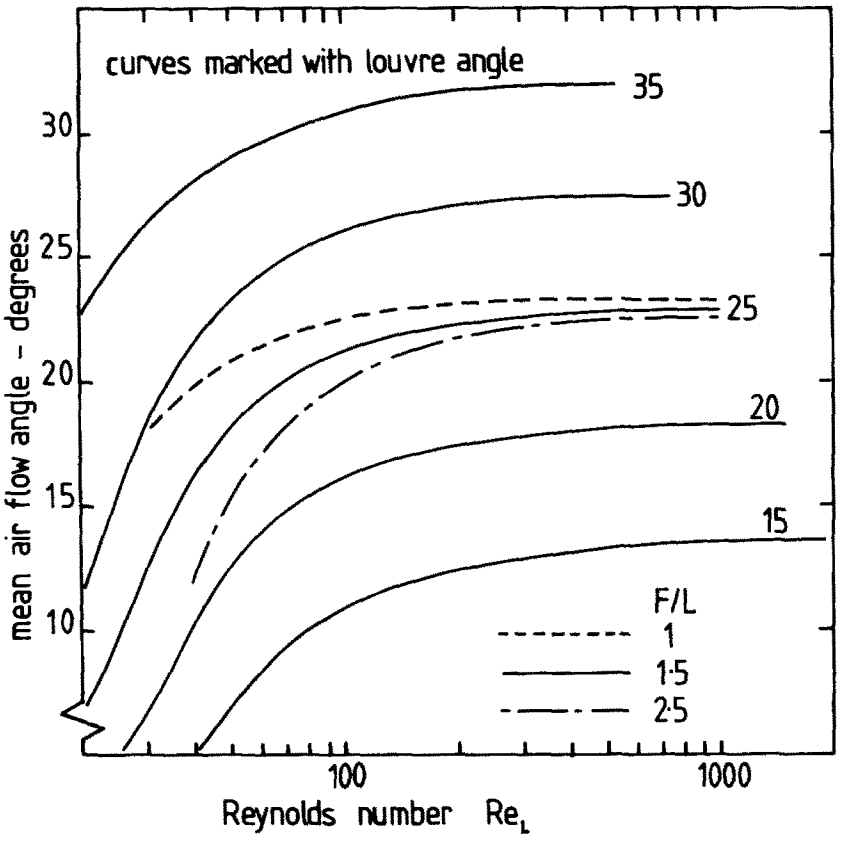

Figure 3. Mean flow angle for fully developed periodic flow through a louver array as a function of Reynolds number and ratio of fin pitch to louver pitch.

a sample with face area approximately 150 mm square for wind tunnel testing.

TEST EQUIPMENT

The wind tunnel for determination of heat transfer and pressure drop characteristics is shown diagrammatically in Fig. 5. The induced flow tunnel is powered by a centrifugal fan that is capable of delivering a velocity of 20 m/s at the 150 mm square test section with the densest test sample in place. Flow is controlled by throttling the fan outlet. For very low velocities, below 5 m/s, flow throttling leads to instabilities, and an alternative axial fan is switched into the duct. This allows stable velocities down to 0.5 m/s to be achieved. In all cases, flow uniformity is found to be better than $2\frac{1}{2}\%$ over the face of the test sample. This allows air velocity to be measured at a single location upstream of the sample using a Pitot tube. To provide a signal for automatic data processing, the Pitot tube is connected to one of two type FC040 transducers from Furness Control. The first has an operat-

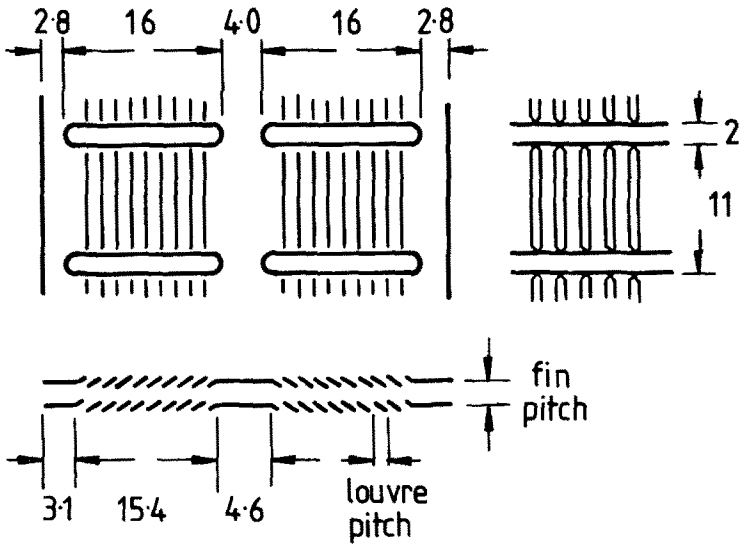

Figure 4. The flat-sided tube and louvered plate fin geometry.

Table 1. Dimensional Details of Variants Tested

Variant	Fin Pitch F (mm)	Louver Pitch L (mm)	Louver Angle α (deg)	Tube Transverse Pitch T (mm)	Rows of Tubes	Hydraulic Diameter d_h (mm)	Min. free flow area frontal area σ
1	2.02	1.4	25.5	11	2	3.33	0.813
2	3.25	1.4	25.5	11	2	4.94	0.822
3	1.65	1.4	25.5	11	2	2.69	0.808
4	2.09	1.4	21.5	11	2	3.37	0.814
5	2.03	1.4	28.5	11	2	3.30	0.813
6	2.15	1.4	25.5	11	1	3.47	0.813
7	1.70	1.4	25.5	11	1	2.76	0.807
8	2.11	0.81	29	11	2	3.38	0.812
9	1.72	0.81	29	11	2	2.81	0.807
10	3.33	0.81	29	11	2	5.02	0.820
11	2.18	1.1	30	11	2	3.49	0.813
12	2.16	0.81	20	11	2	3.45	0.812
13	2.16	1.1	28	8	2	3.14	0.746
14	2.17	1.1	22	14	2	3.66	0.850
15	2.17	1.1	22	8	2	3.16	0.747

σ = ratio of minimum free-flow area to frontal area.

ing range of 0–3 mmH_2Og for measurement of low air velocities, and the other a range of 0–20 mmH_2Og for high-velocity measurement. These were calibrated against inclined tube water manometers.

Air temperature differential across the sample was measured by a 2 × 9 junction thermopile grid made up of chromel-alumel thermocouples. The use of nine junctions for each side yielded two advantages. The first is the large signal for improved accuracy, and the second is automatic averaging of the air temperature distribution from the outlet face. The air inlet temperature was measured relative to the water inlet temperature using a differential thermocouple. The water inlet temperature was measured directly by a chromel-alumel thermocouple using an electronic cold junction. The air-side pressure drop across the sample was measured from pressure tappings upstream and downstream, which were connected to a further FC040 pressure transducer with operating range 0–250 mmH_2Og.

Water was heated in a 450-liter reservoir with three 7.5 kW electric heating elements, and the thyristor controller maintained the water temperature within 0.2 K. A fixed water flow rate of 1.8 kg/s was supplied by a type 114

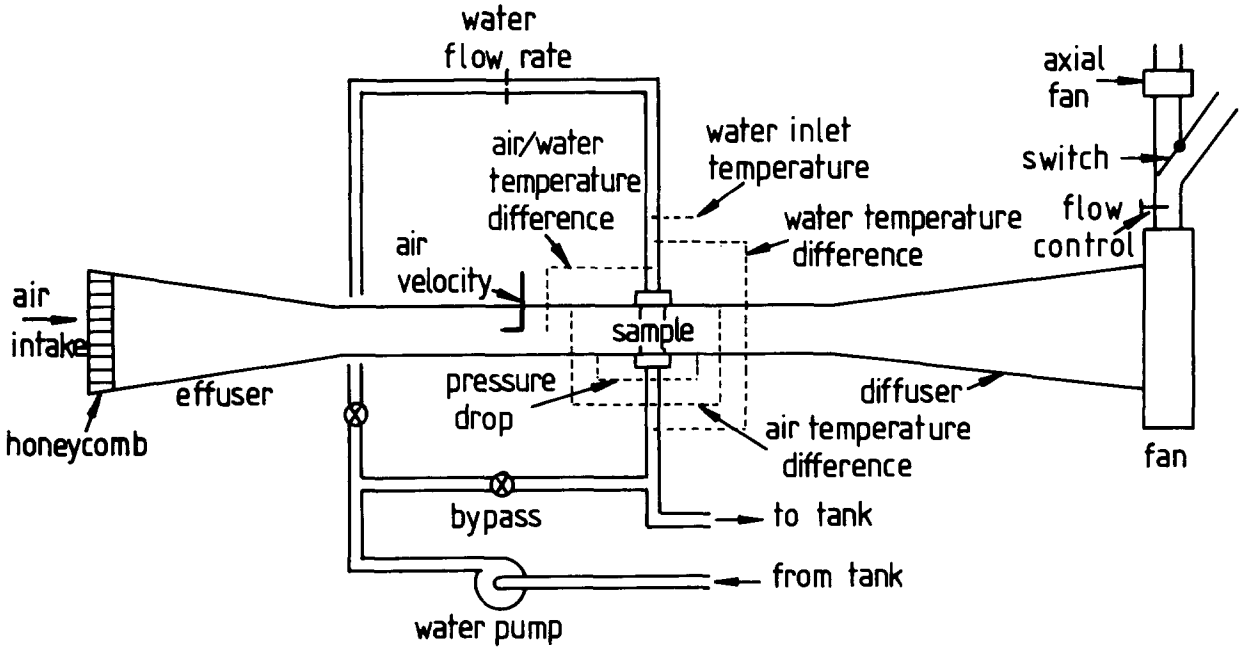

Figure 5. Wind tunnel for measurements of heat transfer and pressure drop characteristics.

Stuart centrifugal pump. Fine control of the flow rate was achieved by adjustment of valves in the main and bypass circuits. Flow rate was measured by orifice plate, the pressure tapping being taken to a DELTAP1 model E-AA transducer, again to allow automatic data collection. The flow rate measurement system was calibrated gravimetrically with water at its operating temperature of 85°C. Water temperature difference was determined by a 2 × 4 junction thermopile of chromel-alumel thermocouples. All thermocouples were calibrated against standard thermometers.

The signals from all transducers were brought to a 3D Inlab A/D converter. The pressure transducer signals were converted directly. Thermocouple signals were taken before conversion to amplifiers with individually adjustable gain controls. The signals from the A/D converter were taken to a BBC microcomputer for future processing. Inlet and outlet temperatures were calculated together with flow rates and air-side pressure drop. Heat flows from the water and to the air were calculated. The data and heat balance were updated and displayed every 3 s.

A water flow rate of 1.8 kg/s and an inlet temperature of 85°C were used in all cases. Measurements were taken for a range of air velocities from 0.5 to 20 m/s. The tunnel was considered to be stable when the mean heat balance over a 1 min period was better than 3%. The average experimental data over the next 1 min period were then stored on disk for later analysis. The next air velocity value was then selected.

After completion of the experimental measurements, values of air-side Reynolds number, Stanton number, and friction factor were calculated. The conventions used by Kays and London [1] were followed throughout. Reynolds number could be based on hydraulic diameter defined as

$$d_h = \frac{4A_c L_s}{A} \tag{1}$$

where A_c is minimum free flow area, L_s is heat transfer matrix depth in the air flow direction, and A is total area for heat transfer on the airside.

An alternative Reynolds number based on louver pitch as the characteristic length proved to be of value in the later correlating procedure. Both Reynolds numbers are based on air velocity through the minimum free flow area.

Stanton number is based on the heat transfer coefficient related to the total heat transfer area, and the mass velocity through the minimum free-flow area. It was calculated by extracting the water-side term, the wall term, and the fin efficiency effect from the overall thermal resistance in the standard way [1]. The water-side term was based on the Dittus-Boelter correlation for turbulent flow inside tubes. At the high water flow rate used here, the water-side thermal resistance was less than 10% of the total in all cases.

The friction factor is defined on the usual basis of "equivalent shear force" per unit total heat transfer area [1]. Again the appropriate velocity is that through the minimum free-flow area. Values were determined from measurements with the sample at ambient temperatures after subtracting the inlet contraction and outlet expansion losses using the appropriate relationships as given in Kays and London [1].

A detailed error analysis suggested that at low Reynolds numbers, values of Stanton number and friction factor are accurate to within 6.5% and 15%, respectively. At the high Reynolds number end, these reduce to 3.5% and 5%, respectively. More details of the test equipment, the analysis procedure, and the error analysis are given in Ref. 9.

EXPERIMENTAL RESULTS

The experimentally determined values of Stanton number (St) and friction factor (f) plotted against Reynolds number (Re) based on hydraulic diameter are displayed in Figs. *6a–e*. Curves are marked with the number of the geometric variant for which the details are given in Table 1. The somewhat idiosyncratic distribution of the curves between the graphs is intended to reduce overlap and improve clarity. The experimental data points are omitted, again for reasons of clarity. Each test represents 17 or more data points each for St and f. In all cases where two samples of a variant were produced, agreement between the results was found to be within 5%. The curves given here represent the best lines through both sets of data points.

Consideration of the friction factor results shows that in all cases the curves have a similar basic shape. On the usual log-log plot, at low Re they have a common steep gradient, which gradually reduces as Re increases. At the high Re end, the gradient again seems to assume a more or less common value.

The Stanton number curves are quite different in shape. At high Re they have a common slope, but as Re is reduced the negative slope reduces to a greater or lesser extent. Many of the curves eventually acquire positive slope (variants 3, 5, 8, 9, 11, 13), and St actually falls as Re is reduced. In the final group (variants 10, 12, 15), the Stanton number slope becomes negative again as the Reynolds number is further reduced.

The question must be asked as to whether these Stanton number phenomena at low Re are genuine. Variant 10 showed the greatest deviation from the straight line. Detailed examination of the experimental results showed an effectiveness of only 0.65 at the lowest air velocity. This value can give no serious problem of experimental accuracy. Other samples have much higher values; for example, for variant 11, the effectiveness is 0.96 at the lowest velocity. Further evidence that the effect is genuine comes from consideration of the experimental values of air temperature at the outlet from the sample. Normally one expects that for fixed values of the other parameters the air outlet temperature will increase as air velocity is reduced. Figure 7 shows how for variant 10 the air outlet temperature falls by some 5 K and then rises again as velocity is reduced over a relatively small velocity range. This result proved to be highly repeatable. The Stanton number behavior is obviously genuine.

As indicated earlier, it has been suggested [7] that Stanton number flattening effects at low Re arise as a result of the fact that, in the extremes, flow can take place either through the gaps between louvers and thus essentially parallel to the louver plane or through the gaps between fins and thus essentially parallel to the fin plane. In reality, the flow pattern moves between these extremes. The Stanton number flattening occurs as the flow switches from louver-directed to fin-directed (Fig. 2) at low Re.

One would expect the nonpreferred flow direction parallel to the fins to be more likely to occur at high values of fin pitch and low values of louver pitch and louver angle. It is therefore significant that the samples showing the largest effect (variants 10 and 12) both have the smallest louver pitch (0.81 mm). Variant 10 also has large fin pitch (3.3 mm), and variant 12 has low louver angle (20°).

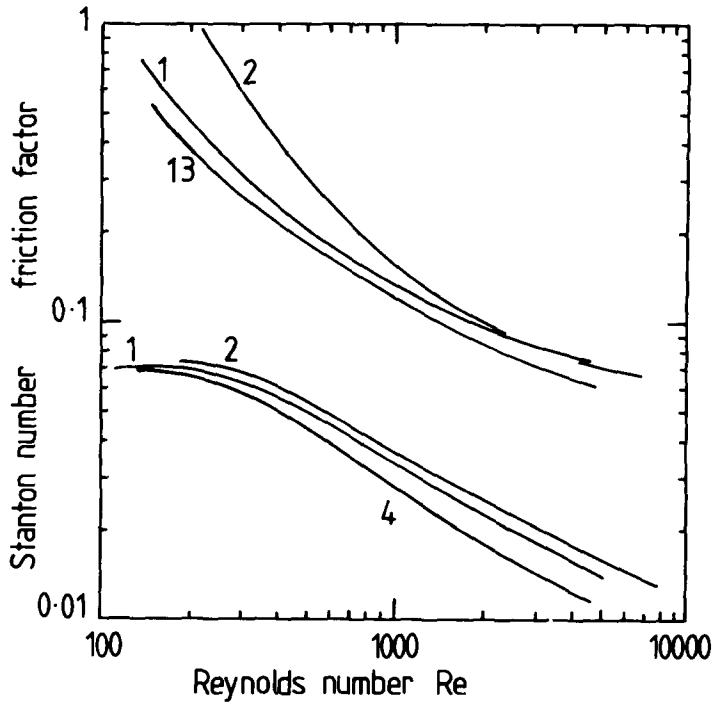

Figure 6(*a*)

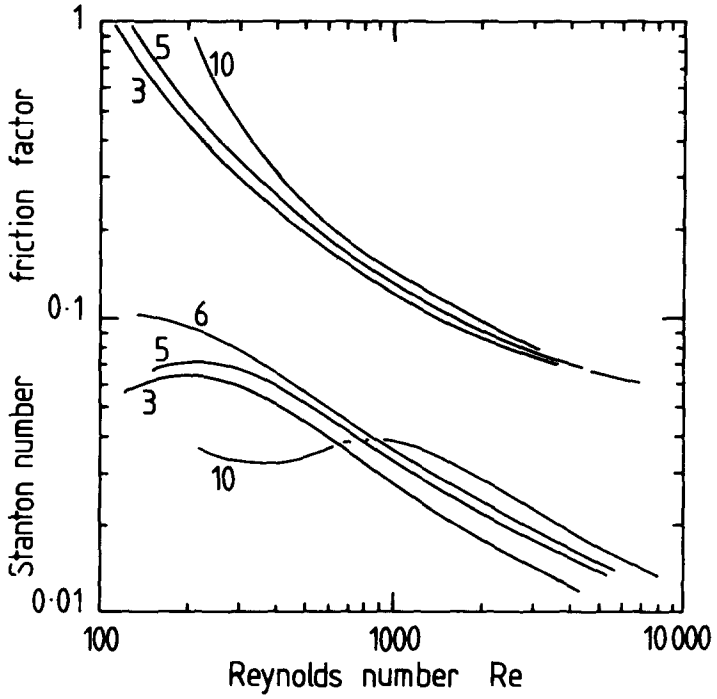

Figure 6(*b*)

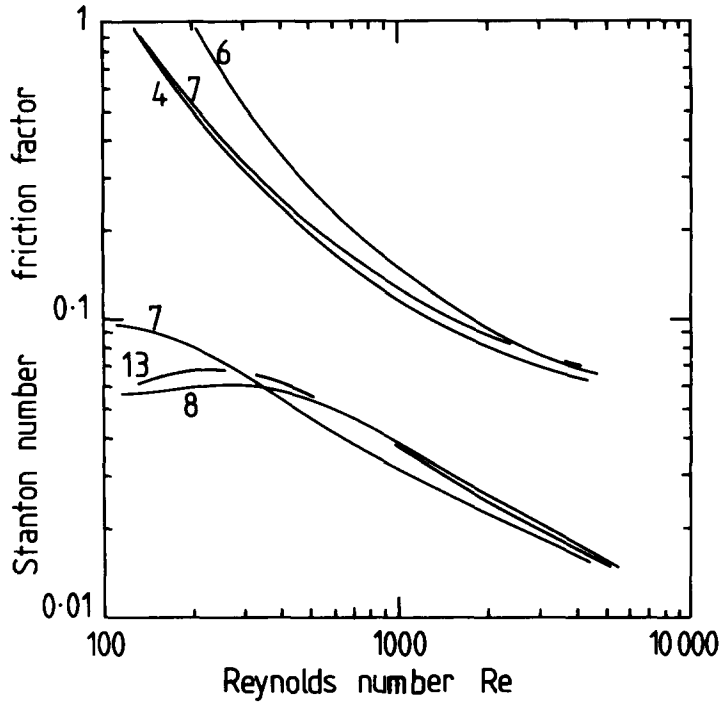

Figure 6(*c*)

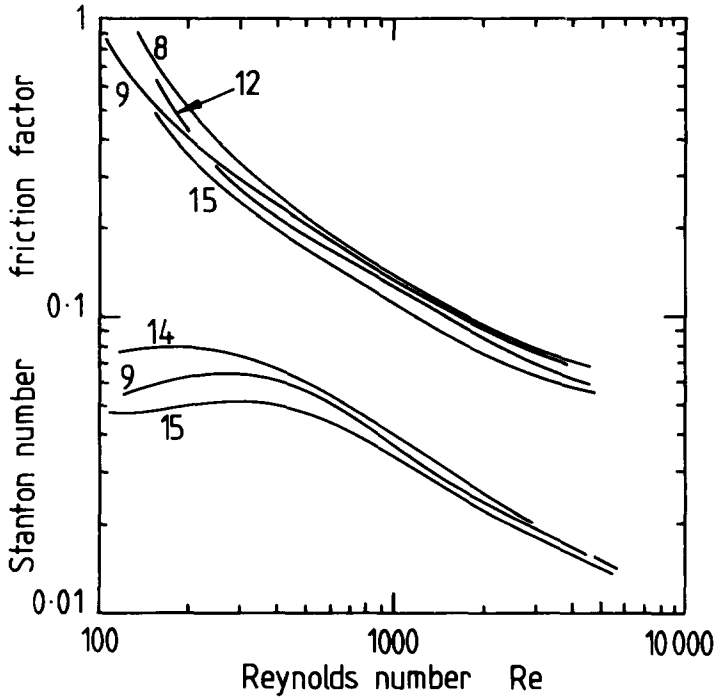

Figure 6(*d*)

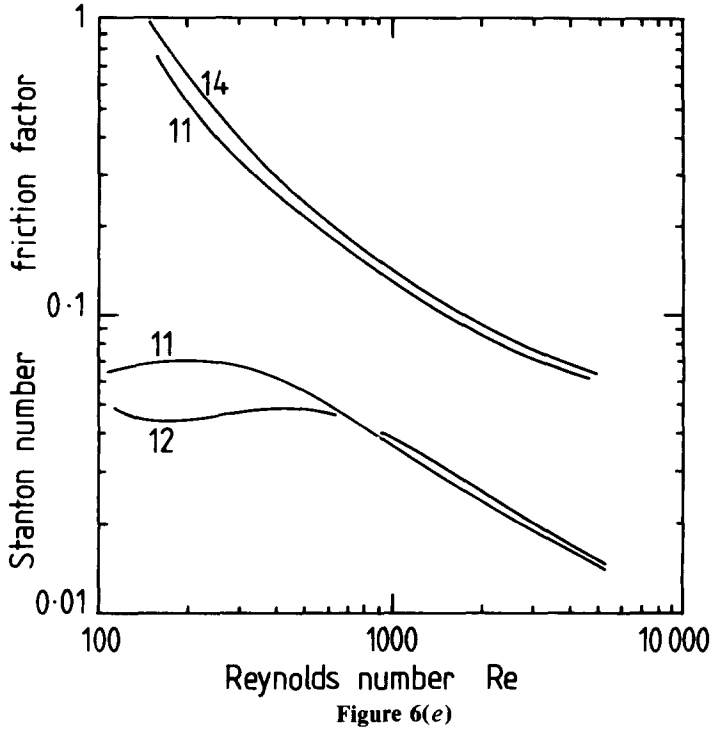

Figure 6(*e*)

Figure 6. Experimental values of Stanton number and friction factor plotted against Reynolds number based on hydraulic diameter. Curves identified with variant number (Table 1).

CORRELATION OF RESULTS

As a result of the very different characteristics of the Stanton number and f curves, different methods of correlation were required for each.

Stanton Number Correlation

It is obvious from consideration of the curves shown in Fig. 6 that no single curve of the traditional form can be expected to describe the complex behavior of the Stanton number. However, a single equation describing the high Re end of the data is possible. It was found that far better correlation could be achieved by basing Reynolds number on louver pitch rather than hydraulic diameter. This is not surprising, because the louvers are behaving like an array of flat plates of length equal to the louver pitch at high Re. The best resulting equation for Re values based on louver pitch, Re = 150–3000, is

$$\mathrm{St} = 1.54\ \mathrm{Re}_L^{-0.57} \left(\frac{F}{L}\right)^{-0.19} \left(\frac{T}{L}\right)^{-0.11} \left(\frac{H}{L}\right)^{0.15} \qquad (2)$$

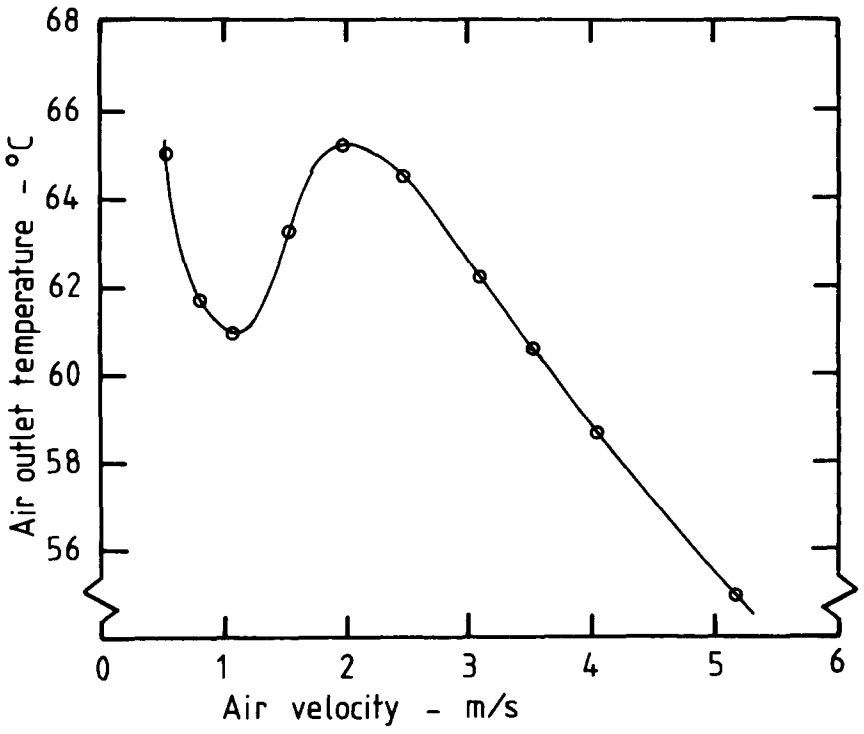

Figure 7. Plot of air outlet temperature as a function of air velocity for sample 10.

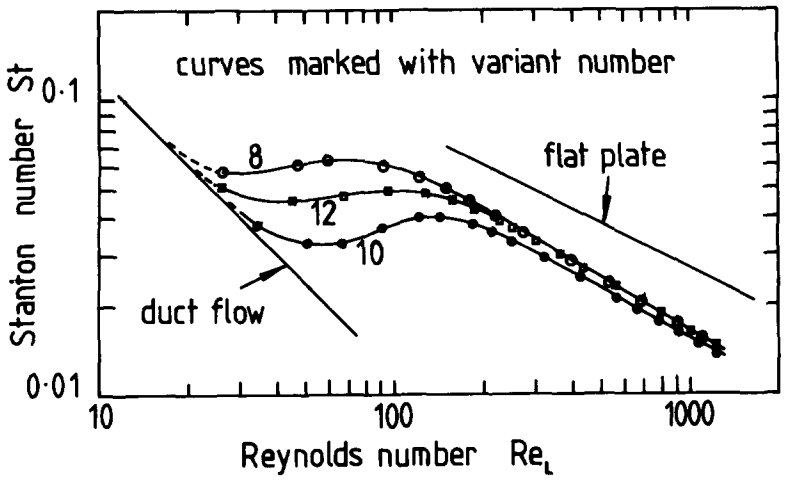

Figure 8. Stanton number curves for variants 8, 10, and 12, demonstrating transition from duct to flat-plate flow.

where F is fin pitch, L is louver pitch, T is transverse tube pitch, and H is louver height given by

$$H = L \sin \alpha \tag{3}$$

where α is louver angle. Number of tube rows was found not to have any significance in this or in any of the later correlations.

This equation yields a regression coefficient of 0.98 and gives St values to within 10%. The Reynolds number power is not far from the Pohlhausen value of 0.5 for flow over a flat plate. In all cases the power to which the nondimensional parameter ratios are raised is relatively small but significant.

It has been suggested that toward the low Re end of the range the flow undergoes a transition from louver direction to fin direction. If this is the case, then the heat transfer characteristics should undergo a transition from flat plate behavior to that appropriate to duct flow. This idea is supported by the curves plotted in Fig. 8. The experimental curves are for variants 8, 10, and 12, which all have 0.81 mm louver pitch. Reynolds number is based on louver pitch, and this time the experimental data points are shown. It can be seen how, at the high Re end, the curves are almost parallel to the Pohlhausen equation for flow over an isolated flat plate. The curves seem to approach the equation for fully developed duct flow at the lowest Re for each test. The curve plotted is for a Nusselt number equal to 4.5, which is the value appropriate to rectangular passages with an aspect ratio equal to 3.3. The samples have passage aspect ratios varying from 2.7 to 4. It can thus be clearly seen that the Stanton number curves are consistent with a transition from duct flow to flat plate flow.

These considerations suggest a possible method for improvement of the equation describing Stanton number as a function of Reynolds number. The Stanton number can be considered as the sum of two components:

$$\mathrm{St} = (1-\gamma)\mathrm{St}_d + \gamma \mathrm{St}_p \tag{4}$$

where St_d is the duct flow component, St_p is the plate flow component, and γ is a function that increases from zero to unity as Re increases. γ obviously also needs to be some function of the geometrical parameters. A solution has been found that makes use of the theoretical results given in Fig. 3, taken from Ref. 9. A simple polynomial equation was developed to describe the ratio of mean flow angle to louver angle as a function of louver angle, the ratio of fin pitch to louver pitch, and Re:

$$\beta/\alpha = (0.936 - 243/\mathrm{Re}_L - 1.76F/L + 0.995\alpha)/\alpha \tag{5}$$

where β is the mean fluid flow angle in degrees.

It is clear that the ratio of mean flow angle to louver angle is a measure of the extent to which the flow is down the duct or over the louvers. It also has the characteristic that its values approach 1 as Re increases. The correlating procedure was therefore repeated setting $\gamma = \beta/\alpha$, and taking all data for Re > 75. For simplicity, the duct flow component of Stanton number was ignored, since it is negligible at Reynolds numbers of practical interest. The improved equation is

$$\mathrm{St} = \frac{\beta}{\alpha} 1.554 \qquad \mathrm{Re}_L^{-0.59} \left(\frac{T}{L}\right)^{-0.09} \left(\frac{F}{L}\right)^{-0.04} \tag{6}$$

The regression coefficient was again 0.98. The H/L term has disappeared, and the exponent of F/L has become very small. The T/L term has also become less significant. This suggests further simplification of the correlation by excluding the effects of the geometrical parameters altogether to yield

$$\mathrm{St} = \frac{\beta}{\alpha} 1.18 \qquad \mathrm{Re}_L^{-0.58} \tag{7}$$

Despite loss of the T/L term, this expression still has a regression coefficient of 0.97. This simple equation is found to describe all the Stanton number data for $\mathrm{Re}_L > 75$ to within 10%.

Friction Factor Correlation

Consideration of the friction factor results showed that in all cases the slope of the curves plotted on a log-log basis changes continuously from a value approximately equal to -1 at low Re to a value around -0.3 at the high Re end. When plotted against a louver pitch Reynolds number, it is clear that the slope is very largely a function of Re alone. It is also found that f values range from 30% to over 100% above the values given by the Blasius equation for flow over a flat plate. This presumably is because of the duct flow phenomenon at low Re values and because of an increasingly significant form drag component of the fluid resistance at the high Re end.

The continuously changing slope of the friction factor curves means that correlating equations of the standard form cannot

be developed. As a first step in arriving at a solution to this problem, all the experimental data were used to derive a polynomial equation for average friction factor as a function of Re alone. The second-order polynomial is

$$\log f_A = 2.775 - 2.25 \log \mathrm{Re}_L + 0.318 (\log \mathrm{Re}_L)^2 \quad (8)$$

Rearrangement of this equation yields

$$f_A = 596\ \mathrm{Re}_L^{(0.318 \log \mathrm{Re}_L - 2.25)} \quad (9)$$

The value of this parameter f_A can be calculated from the value of Re_L for any data point and can be used in a correlation exercise in the normal way instead of the parameter Re_L. Attempts were made to derive correlations using all possible nondimensional combinations of the geometric variables, but it was found that satisfactory accuracy could only be achieved with the use of dimensional parameters. The final equation for the friction factor is

$$f = 0.895 f_A^{1.07} F^{-0.22} L^{0.25} T^{0.26} H^{0.33} \quad (10)$$

where all dimensions are in millimeters.

Equation (10) predicts friction factors to within 10% for values of Re between 150 and 3000. For $\mathrm{Re} < 150$, it is found that a simple relationship of the standard form can be derived. The result is

$$f = 10.4\ \mathrm{Re}_L^{-1.17} F^{0.05} L^{1.24} H^{0.25} T^{0.83} \quad (11)$$

The correlation coefficient is 0.91. The slope of -1.17 is close to the expected value for duct flow (-1).

CONCLUSIONS

This paper represents the first publication of comprehensive performance data for flat tube and louvered plate fin surfaces. The data cover the Reynolds number range from 120 to 8000 for the heating of air at ambient temperatures. The extremely complex behavior demonstrated by the Stanton number curves has been explained in terms of transition from a "flat plate" to a "duct flow" characteristic as Reynolds number is reduced. It occurs when the boundary layers building up on the louver leading edges become thick enough to effectively block off the gap between adjacent louvers in a fin. Earlier workers [7] suggested that this is a cause of flattening of the Stanton number curve as Reynolds number is reduced. This is confirmed, and the effect is conclusively demonstrated here for the first time. The results of a theoretical description of the flow patterns through louver arrays [9] have been used to help derive simple and accurate correlating equations. These can be used for fin design.

The recognition of the possibility of duct flow at low Re is important for the fin designer. In recent years the trend has been toward ever-reducing louver pitch in order to introduce more leading edges and thus increase mean heat transfer coefficients. However, as the results here demonstrate, the danger exists of inducing the nondesired "duct flow" too far up the velocity range, particularly if small louver pitch is combined with large fin pitch and/or small louver angle. The results given here allow the designer to avoid this danger.

The correlations presented here were developed from measurements on samples at a scale that is representative of that used in industry, and as such they are highly applicable to the optimization of heat transfer surface designs in the region of the geometric range covered by the experimental program. The correlations have already been used to design production fins that yield very significant performance advantages over existing designs.

The authors would like to thank Covrad Heat Transfer for their contribution to this program of work. Out gratitude is also due to Ford Motor Company, whose generous support for the department's wider research program made available the test equipment used in the work described here.

NOMENCLATURE

A	Total area for heat transfer, m^2
A_c	Minimum free flow area, m^2
c_p	Specific heat capacity, J/(kg K)
d_h	Hydraulic diameter, Eq. (1), m
F	Fin pitch, mm
f	Fanning friction factor, dimensionless
f_A	Correlating parameter in Eqs. (8)–(10), dimensionless
G	Mass velocity through minimum free-flow area, $kg/(m^2\ s)$
h	Heat transfer coefficient, $W/(m^2\ K)$
H	Louver height, mm
L	Louver pitch, mm
L_s	Heat transfer matrix depth in airflow direction, m
N_{tu}	Number of heat transfer units, dimensionless
Re	Reynolds number based on hydraulic diameter ($=d_hG/\mu$), dimensionless
Re_L	Reynolds number based on louver pitch ($=LG/\mu$), dimensionless
St	Stanton number ($=h/Gc_p$), dimensionless
St_d	Stanton number arising from duct flow, Eq. (4), dimensionless
St_p	Stanton number arising from flat plate flow, Eq. (4), dimensionless
T	Tube transverse pitch, mm

Greek Symbols

α	Louver angle, deg
β	Mean flow angle through louver array, deg
γ	Function in Eq. (4)
μ	Dynamic viscosity, Pa s
σ	Ratio of minimum free flow to frontal area, dimensionless

REFERENCES

1. Kays, W. M., and London, A. L., *Compact Heat Exchangers,* 2nd ed., McGraw-Hill, New York, 1984.
2. Davenport, C. J., Heat Transfer and Flow Friction Characteristics of Louvered Heat Exchanger Surfaces, in *Heat Exchangers: Theory and Practice,* J. Taborek, G. F. Hewitt, and N. Afgan, Eds., pp. 397–412, Hemisphere/McGraw-Hill, Washington, D.C., 1983.
3. Beauvais, F. N., An Aerodynamic Look at Automotive Radiators, SAE Paper No. 650470, 1965.
4. Smith, M. C., Gas Pressure Drop of Louvered Fin Heat Exchangers, ASME Paper No. 68-HT-27, 1968.
5. Smith, M. C., Performance Analysis and Model Experiments for

Louvered Fin Evaporator Core Development, SAE Paper No. 720078, 1978.
6. Wong, L. T., and Smith, M. C., Air-Flow Phenomena in the Louvered-Fin Heat Exchanger, SAE Paper No. 730237, 1973.
7. Davenport, C. J., Heat Transfer and Fluid Flow in Louvred Triangular Ducts, Ph.D. Thesis, CNAA, Lanchester Polytechnic, 1980.
8. Shah, R. K., and Webb, R. L., Compact and Enhanced Heat Exchangers, in *Heat Exchangers: Theory and Practice,* J. Taborek, G. F. Hewitt, and N. Afghan, Eds., pp. 425–468, Hemisphere/McGraw-Hill, Washington, D.C., 1983.
9. Achaichia, A., The Performance of Louvred Tube-and-Plate Fin Heat Transfer Surfaces, Ph.D. Thesis. CNAA, Brighton Polytechnic, 1987.
10. Achaichia, A., and Cowell, T. A., Fully Developed Periodic Flow in Inclined Louvre Arrays, in preparation.